

Adsorption of heavy metal ions using semi-coke derived from pyrolysis of coal

Xinhao Wang, Zhengfeng Liu, Jiajia Zhang, Jiamei Zhu*, Shuangquan Zhang*

School of Chemical Engineering and Technology, China University of Mining and Technology, Xuzhou 221116, China, emails: zhujamei@hotmail.com (J. Zhu), cumtzsq@126.com (S. Zhang), wang19851620865@163.com (X. Wang), lzfvoy12@163.com (Z. Liu), 1437443437@qq.com (J. Zhang)

Received 1 January 2020; Accepted 21 July 2020

ABSTRACT

Aiming to reduce the treating cost of an aqueous solution containing heavy metal ions, a semi-coke adsorbent, a kind of waste produced from coal pyrolysis was prepared and the characteristics were investigated. The results have shown that surface area of semi-coke power increased with the increase of pyrolysis temperature (600°C–800°C), while the density of acid and basic functional groups per unit area was the highest at 600°C. The adsorption properties of heavy metal ions were further estimated. Isothermal adsorption was fitted by the Freundlich model and kinetics confirmed to pseudo-second-order kinetic model. Adsorption capacity determined by dynamic experiment was 41.15 mg/g for Cr³⁺, 7.58 mg/g for Ni²⁺, 37.03 mg/g for Cu²⁺, 1.97 mg/g for Cd²⁺, and 129.70 mg/g for Pb²⁺. X-ray photoelectron spectroscopy analysis indicated that surface functional groups including C–O, NH₂, pyrrole, pyridine, and thiophene were involved in the adsorption process, resulting in enhanced adsorption capacity.

Keywords: Adsorption; Aqueous solution; Dynamic; Thermodynamic; Heavy metal

1. Introduction

Heavy metal ions are one of the toxic substances that seriously pollute the environment and threaten public health [1], so it is greatly necessary to develop a highly efficient remediation technology. There are many chemical and physicochemical methods including adsorption, chemical precipitation, electrochemical reduction, and ion exchange, and so on for the treatment of water polluted by heavy metal ions [2], among them adsorption as a simple and effective technology is most commonly used.

Activated carbon (AC) as a common adsorbent has become a research focus in the treatment of heavy metal pollutants [3–5] due to the developed porosity and huge specific surface area. Many researches recently have also been focused on the development of more effective and cheaper adsorbents. Biochar which is a carbonized material

generated from pyrolysis of biomass under lack of oxygen is an environment-friendly adsorbent. As a bright prospect adsorbent for reducing heavy metal ion contaminants, it has attracted substantial attention, and the adsorption capacity of biochar obtained from agricultural residues, animal wastes, and woody materials has been investigated [6–8]. However, the high prices still make current materials less suitable for spreading the adsorption technology to remove heavy metals on an industrial scale.

China and the United States, along with Russia, have the world's largest coal reserves. Semi-coke is a kind of waste produced in the process of coal pyrolysis and produced about 100 million tons annually in China. Semi-coke which has the advantage of rich resources and extremely low price is mainly used as an energy source by combustion, thus the comprehensive utilization of semi-coke powder is of great significance.

* Corresponding authors.

Semi-coke powder can be as adsorption or catalytic material due to its developed pore structure and abundant oxygen-containing functional groups. Moreover, semi-coke has stable property and not easy to be degraded by microorganisms [9]. Recently, modified semi-coke was used in the field of flue gas desulfurization [10–12]. Yang et al. [13] reported a semi-coke catalyst to remove nitric oxide under visible light. Zhang et al. [14] studied the semi-coke adsorbent for the treatment of mercury vapor. At present, there are few reports of the adsorption property of semi-coke produced by the pyrolysis of coal for heavy metal ions in aqueous solutions. Zhang et al. [15] reported semi-coke powder treated by microwave oven or KOH and H₂O₂ solution could remove effectively Cr⁶⁺ and methylene blue (MB) solution. The specific surface area of modified semi-coke was 84.92 m²/g and the process of Cr⁶⁺ and MB adsorption presented pseudo-second-order kinetics. To develop the semi-coke adsorbent obtained from coal on industrial-scale process, we explored the further application of it for heavy metal ions adsorption, expecting to adjust the pore structure and functional groups on the surface via pyrolysis condition. Therefore, it is inferred that using semi-coke powder from coal pyrolysis as adsorbent can not only reduce the cost of sewage treatment, but also open up a new idea for efficient and clean utilization of waste.

In this work, solid waste material was application to achieve low-cost adsorbent for adsorption heavy metal ions (Cr³⁺, Ni²⁺, Cu²⁺, Cd²⁺, and Pb²⁺) in aqueous solution. The surface functional groups and porosity of the resulting semi-coke powder were characterized. The adsorption experimental data with different ions concentrations were analyzed using kinetic equations and adsorption mechanism was investigated in detail to provide a theoretical basis for large-scale application in the future.

2. Materials and methods

2.1. Samples preparation

Coal (Urumqi, Xinjiang Province) was ground into particle size ≤6 mm and coal sample (50.0 g) was put into a muffle furnace at a rate of about 10°C/min and the terminal pyrolysis temperature was 600°C, 650°C, 700°C, 750°C, and 800°C, respectively. Then the temperature was maintained for 20 min after reaching pyrolysis temperature.

2.2. Characterization of semi-coke

The specific surface area and pore size distribution of N₂ adsorption isotherms at –196°C were measured by Autosorb-1-MP adsorption instrument (Quantachrome, FL, USA). The contents of functional groups on surface of semi-coke were tested by the Boehm titration method [16]. The functional groups on surface of semi-coke were investigated by Thermo Scientific Nicolet 380 FTIR infrared spectrometer (Thermo Scientific, MA, USA). Surface element morphology of semi-coke was analyzed by ESCALAB250Xi X-ray diffraction photoelectron spectroscopy (Thermo Fisher Scientific, MA, USA), and the binding energy was referenced to the neutral C1 speak at 284.8 eV. XPS Peak Fit software (V4.1) was used for spectra fitting.

2.3. Thermodynamic and kinetic adsorption of semi-coke

Single-metal-ion solutions of Cr³⁺, Ni²⁺, Cu²⁺, Cd²⁺, and Pb²⁺ were obtained by dissolving their corresponding nitrate, chloride, or sulfate salts, Cr(NO₃)₃, NiSO₄, CuSO₄, CdSO₄, and PbCl₂, respectively, in deionized water. Dried semi-coke (0.5 g) was added into the temperature controlled conical flask in shaking condition. Then single-metal-ion solution with 0.01 mol/L NaNO₃ as supporting electrolyte was respectively added into the flasks and pH value was regulated to 5.5. The sewage with different ions concentrations were prepared. The initial concentration ranges of Cr³⁺, Ni²⁺, Cu²⁺, Cd²⁺, and Pb²⁺ are 200–1,500, 20–120, 20–200, 1–30, and 200–1,500 mg/L for the equilibrium study and 300, 40, 80, 5, and 300 mg/L for kinetic experiment, respectively. The initial concentrations of heavy metal ions in this study were simulated industrial wastewater containing different concentrations of the metal ions. The mixture containing each metal ion was shaken at 25°C for 4 h in doing the thermodynamic adsorption experiment. After adsorption and filtration, the concentrations of heavy metal ions in the filtrate were determined by inductively coupled plasma mass spectrometry (ICP-MS).

Equilibrium adsorption and the removal efficiency were calculated according to Eqs. (1) and (2), respectively.

$$q_e = \frac{(C_0 - C_e) \times V}{m} \quad (1)$$

$$\eta = \frac{C_0 - C_e}{C_0} \times 100 \quad (2)$$

where q_e is adsorption capacity at equilibrium (mg/g). η is the removal efficiency (%). C_0 and C_e the concentrations at starting and equilibrium (mg/L), respectively. V is the solution volume (L) and m is the mass of the semi-coke (g).

The dynamic adsorptions of heavy metal ions at different time were obtained using Eq. (3).

$$q_t = \frac{(C_0 - C_t) \times V}{m} \quad (3)$$

where q_t is dynamic adsorption capacity (mg/g). C_t is concentration at defined time (mg/L).

3. Results and discussion

3.1. Influence of pyrolysis temperature on semi-coke pore structure

The pore structure parameters of semi-coke powder at different pyrolysis temperature are shown in Table 1. The pore structures of semi-coke samples are mainly composed of micropores, which are beneficial to the adsorption of metal ions. With the increase of pyrolysis temperature, the specific surface area, and microporosity of semi-coke increased at first and then decreased. Semi-coke powder from pyrolysis of coal presents better specific surface area and developed micropore, which is 122.4 m²/g and 61.47% at 700°C, respectively. It indicates that the obtained semi-coke samples may have high adsorption capacity.

Table 1
Pore structure parameters of semi-coke obtained from pyrolysis of coal

Sample	Pyrolysis temperature (°C)	S_{BET} (m ² /g)	V_{mic} (mL/g)	V_t (mL/g)	Microporosity (%)	D_{ave} (nm)
WPC600	600	69.9	0.01339	0.04377	30.59	1.834
WPC650	650	97.2	0.02746	0.05962	46.06	1.543
WPC700	700	122.4	0.03984	0.06481	61.47	1.543
WPC750	750	111.1	0.03266	0.06387	51.14	1.543
WPC800	800	112.3	0.03643	0.06970	52.27	1.543

The effect of pyrolysis temperature on the porosity of semi-coke is very significant, which is due to cleavage of side-chains in the edge of the main coal structure and separating out of small hydrocarbons, such as methane. It further leads to change in both pore structural strength and micropores of semi-coke in process of the coal pyrolysis [17].

3.2. Influence of pyrolysis temperature on the functional groups

The contents of surface functional group of semi-focal from different pyrolysis temperatures are given in Table 2. With the increase of pyrolysis temperature, the phenolic hydroxyl, and carboxyl groups on the surface of semi-coke decreased gradually, especially carboxyl group almost disappeared after 650°C. The main reason is that carboxyl group connected with organic macromolecular is unstable and can crack into CO₂, H₂, or other small molecules under the 250°C–400°C. Compared with COOH, the phenolic hydroxyl group has better stability and the decomposition temperature is usually greater than 650°C [18]. While there is no regularity between the content of lactone group and pyrolysis temperature, which is probably due to the partial decomposition of lactone group with pyrolysis temperature increased, and at the same time, the polycondensation reaction occurred resulting in formation of relatively stable C=O group [19,20].

The adsorption properties of carbonaceous material are related not only to the porosity, but also to the surface functional groups [21]. As shown in Table 2, specific surface area of the semi-coke increases with pyrolysis temperature improved, but the content of surface functional groups decreases. The density of acid and basic functional group per unit area of WPC600 are the highest with the value of 0.00280 and 0.01635 mmol/m² at 600°C, respectively. Zhang et al. [22] investigated that biochar gives better

adsorption capacity for Pb²⁺ in aqueous solution compared with activated carbon because biochar with lower specific surface has higher density of functional group compared with activated carbon. Therefore, semi-coke powder from pyrolysis of coal at 600°C was selected for following adsorption experiment, which might provide more excellent adsorption performance.

3.3. Adsorption performance of semi-coke

3.3.1. Adsorption isotherms

For understanding the interacts between adsorbent and adsorbent surface, adsorption thermodynamics is an important foundation. WPC600 with the highest density of functional group obtained from pyrolysis at 600°C was used to adsorb heavy metal ions. Langmuir monolayer adsorption model (Eq. (4)) and Freundlich multilayer adsorption model [23] (Eq. (5)) were used to describe the adsorption isotherms of semi-coke to Cr³⁺, Ni²⁺, Cu²⁺, Cd²⁺, and Pb²⁺ in solution.

$$\frac{C_e}{q_e} = \frac{1}{q_m K_L} + \frac{C_e}{q_m} \quad (4)$$

$$q_e = \ln K_F C_e^{1/n} \quad (5)$$

where q_e and q_m are adsorption capacity of semi-coke to heavy metal ions at equilibrium and maximum (mg/g). C_e is the solution concentration at equilibrium (mg/L). n is the adsorption intensity. K_L and K_F are Langmuir constants (L/mg) and Freundlich constant (mg/g), respectively.

Fig. 1 presents the adsorption isotherms of semi-coke for heavy metal ions. With the increase of the initial concentration of Cr³⁺, Ni²⁺, Cu²⁺, Cd²⁺, and Pb²⁺, the adsorption

Table 2
Contents of functional groups on semi-coke surface

Sample	Lactone group (mmol/g)	Phenolic hydroxyl (mmol/g)	Carboxyl (mmol/g)	Density of acid functional group (mmol/m ²)	Density of basic functional group (mmol/m ²)
WPC600	0.013	0.168	0.015	0.00280	0.01635
WPC650	0.023	0.142	0.005	0.00175	0.01155
WPC700	0.020	0.126	–	0.00120	0.00842
WPC750	0.037	0.106	0.001	0.00130	0.01042
WPC800	0.008	0.097	–	0.00093	0.01007

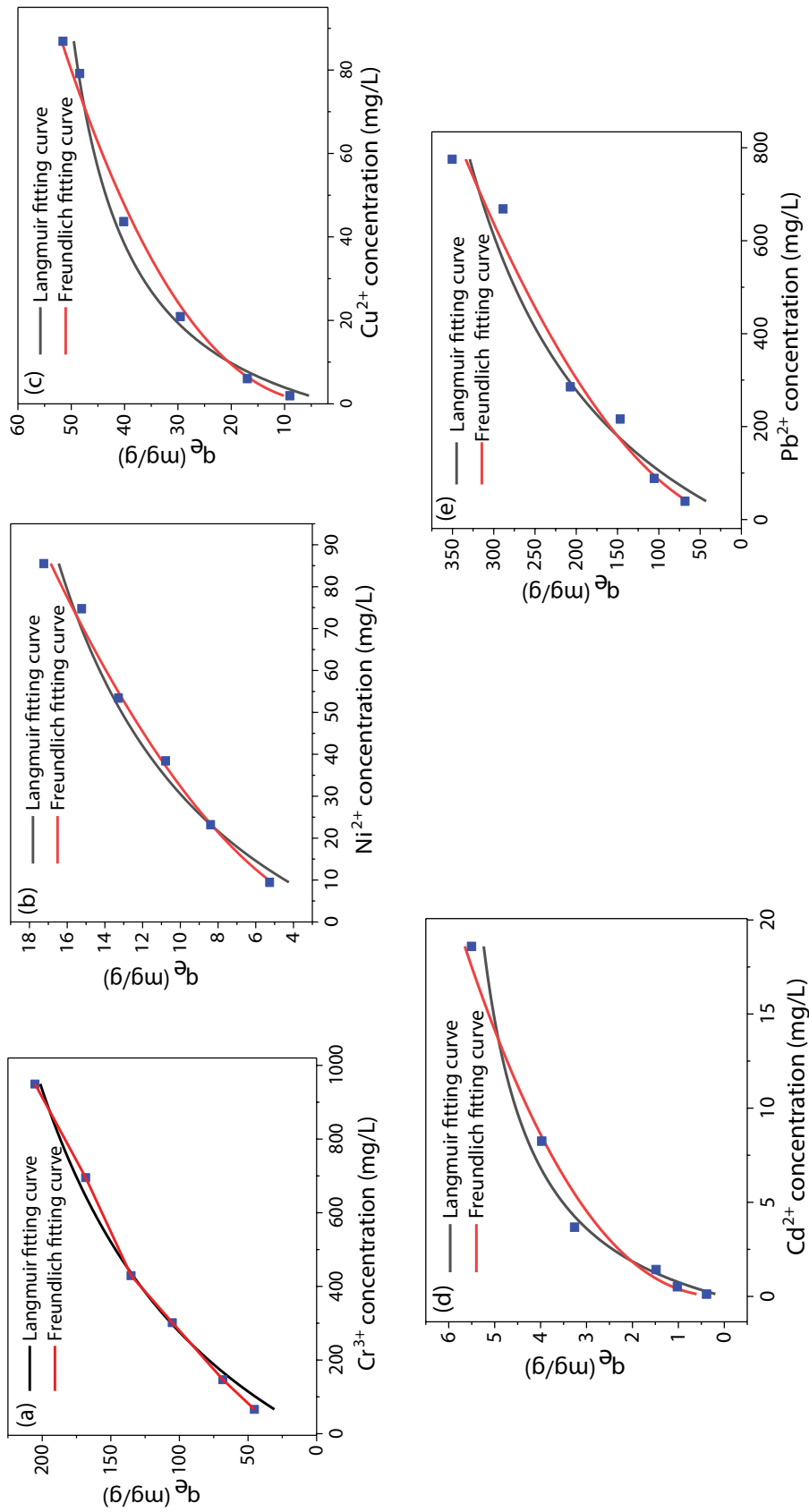


Fig. 1. Adsorption isotherms of semi-coke: (a) chromium(III), (b) nickel(II), (c) copper(II), (d) cadmium(II), and (e) lead(II) fitting by Langmuir and Freundlich model.

capacity increased obviously. When the ion concentration in aqueous solution is higher, it can overcome mass transfer resistance more effectively with stronger ion driving force, thus this is beneficial to the adsorption of ion onto adsorbent surface [24,25]. It is noted that the adsorption curves of Cu^{2+} and Cd^{2+} in high concentration are relatively gentle, which is due to the occupation of surface-active sites of semi-coke resulting in the change of adsorption slowing down.

The relevant parameters of Langmuir and Freundlich fitting equation are shown in Table 3. The theoretical maximum adsorption capacities q_m of Cr^{3+} , Ni^{2+} , Cu^{2+} , Cd^{2+} , and Pb^{2+} are 344.92, 25.61, 60.91, 6.39, and 514.47 mg/g based on the Langmuir equation. Moreover, according to the Freundlich equation, the value of n is used to describe the intensity of adsorption. It proves that Freundlich constant n is an indication of suitability of the system [26] and it is favorable adsorption condition as the value of $n > 1$. Judging from n values of WPC600 for these five heavy metal ions shown in Table 3, it indicates that WPC600 is favorable adsorbent material. For semi-coke, the Freundlich isotherm provides a higher correlation coefficient (R^2) than the Langmuir model. According to the Freundlich model, it shows that the adsorption occurs on the surface of the heterogeneous adsorbent, that is, the active center mainly occurs on the surface of semi-coke.

The removal efficiencies of Cr^{3+} , Ni^{2+} , Cu^{2+} , Cd^{2+} , and Pb^{2+} in solution are also shown in Fig. 2. With improvement of initial concentration of these heavy metal ions for WPC600, the tendency of removal rate decreases gradually, then slightly increases at higher concentration, except Cd^{2+} having better adsorption at lower initial concentration.

The removal efficiencies for Cr^{3+} , Ni^{2+} , Cu^{2+} , Cd^{2+} , and Pb^{2+} are 63.58%, 52.65%, 90.26%, 82.78%, and 80.23%, when the concentrations of all metal ions are 200, 20, 20, 3, and 200 mg/L, respectively. The differences in removal ability among them are caused by the different hydration radius and hydration energy of cations [27].

3.3.2. Adsorption kinetics

In the process of adsorption, both adsorption isotherm and kinetics should be investigated. The kinetic curves of Cr^{3+} , Ni^{2+} , Cu^{2+} , Cd^{2+} , and Pb^{2+} onto WPC600 are depicted in Fig. 3. During the beginning of adsorption, the adsorption rate obviously improves. With the increase of adsorption time, the rate gradually slows down and reaches equilibrium after 4 h.

The adsorption rate of semi-coke on heavy metal ions is usually determined by liquid phase or intraparticle mass transfer rate. Three stages could be usually involved in the process of metal ions adsorption by WPC600. In the first stage, it can be attributed to the external surface adsorption, that is, the adsorption diffuses to the outer surface of the adsorbent through the solution or the boundary layer diffusion of solute molecules with higher adsorption rate. In the second stage, the adsorption rate gradually slows down and it is mainly controlled by the intra-particle diffusion process. The third stage is the adsorption equilibrium stage. When the concentration of heavy metal ions in the solution is very low or the adsorbate reaches the maximum adsorption capacity, the diffusion in the particles begins to slow down and tends to stabilize [28]. Finally, adsorption reaches equilibrium.

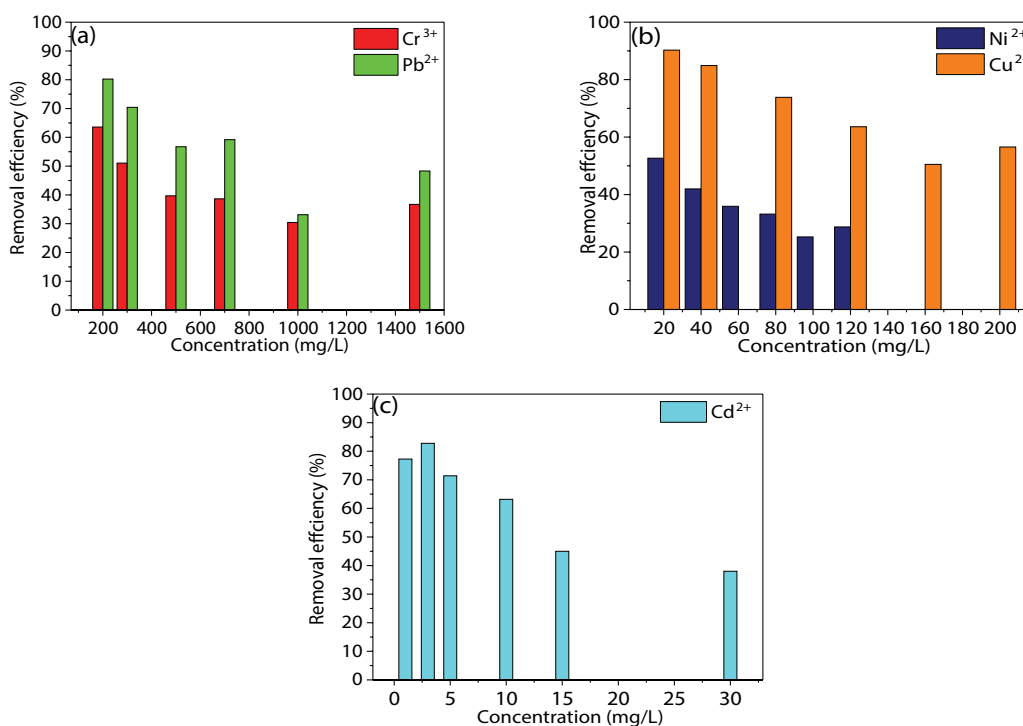


Fig. 2. (a–c) Removal efficiency of heavy metals by semi-coke.

Table 3
Related parameters of Langmuir and Freundlich fitting equations

Ions	Langmuir model			Freundlich model			
	q_m (mg/g)	K_L (L/mg)	R^2	S_L	K_F (mg/g)	n	R^2
Cr ³⁺	344.92	0.0015	0.9588	0.77	4.08	1.75	0.9971
Ni ²⁺	25.61	0.0201	0.9704	0.71	1.54	1.86	0.9964
Cu ²⁺	60.91	0.0501	0.9161	0.50	7.62	2.33	0.9557
Cd ²⁺	6.39	0.2454	0.8978	0.80	1.52	2.23	0.9709
Pb ²⁺	514.47	0.0023	0.8995	0.68	8.76	1.83	0.9656

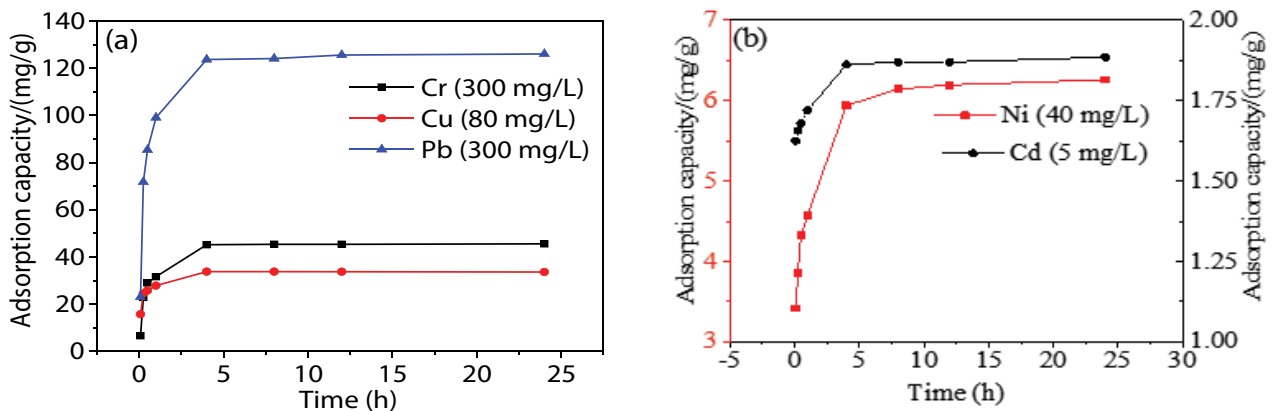


Fig. 3. (a and b) Adsorption kinetic curves of heavy metals on semi-coke.

The Lagergren pseudo-first-order and pseudo-second-order models are usually used to describe the adsorption characteristics on the adsorbent surface [29]. The expressions are as follows:

$$\log(q_e - q_t) = \log q_e - \frac{k_1}{2.303} t \quad (6)$$

$$\frac{t}{q_t} = \frac{1}{K_2 q_e^2} + \frac{1}{q_e} t \quad (7)$$

where t is the time (h) and q_t is adsorption of t time (mg/g). k_1 is the reaction rate constant of first-order kinetic equation (1/h) and k_2 is the reaction rate constant of two order kinetic equation (g/(mg h)).

The relation diagrams between t/q_t and t of metal ions adsorbed by WPC600 are shown in Fig. 4 and the kinetic parameters determined from the curves are listed in Table 4. The correlation coefficients derived from the pseudo-second-order equation are greater than 0.95, which are much higher than those of the pseudo-first-order equation. This suggests that the adsorption process obeys the pseudo-second-order kinetic model. Based on the pseudo-second-order dynamic equation, the adsorption capacity at equilibrium q_e and actual adsorption capacity are very close, which also indicates that kinetics data of semi-coke for Cr³⁺, Ni²⁺, Cu²⁺, Cd²⁺, and Pb²⁺ are good for the pseudo-two-order model and the adsorption process is dominated by chemisorption [30].

Adsorption capacity estimated by pseudo-second-order dynamic equation of semi-coke in this work was compared with the values in literatures. Comparison of the $q_{e,cal}$ values of various adsorbents for Cu²⁺ and Pb²⁺ ions were shown in Table 5. Biochar samples derived from date seeds [31], sewage sludge [32], earthworm manure (EMBC-400) [24], green macroalgae (E and EW) [33], *Prosopis africana* shell [34], wheat straw [35], pigeon peas hulls [36], pinewood [37], and orange peel [38] were used to adsorb Cu²⁺ and adsorption capacity of $q_{e,cal}$ at equilibrium are 9.6, 7.32, 18.33, 29.6, 95.2, 31.3, 4.3, 20.8, 3.9, and 3.65 mg/g, respectively. The adsorption value of WPC600 in this study for Cu²⁺ ion is relatively high (36.74 mg/g). Compared with the biomass generated from fresh and dehydrated banana peels (14.88 and 15.11 mg/g) [25], water hyacinths (47.33 mg/g) [39], sugar cane bagasse (45.80 mg/g) [40], Chinese medicine material residue the (MBC400) (96.5 mg/g) [41], peanut shell (PBC400) (56.9 mg/g, 4) [41], *Alternanthera philoxeroides* (52.55 mg/g) [42], sewage sludge (30.88 mg/g) [43], activated carbon derived from *Polygonum orientale* Linn (102.02 mg/g) [44], and orange peel (7.75 mg/g) [38], the adsorption capacity of WPC600 for Pb²⁺ ion (128.21 mg/g) is much higher. Therefore, cheap semi-coke derived from pyrolyzed of coal is effective for adsorption of heavy metal ions solution, especially for polluted-water containing Cu²⁺ and Pb²⁺ ions.

3.4. Adsorption mechanism

The insight into the mechanism of before and after semi-coke adsorption of heavy metal ions were determined

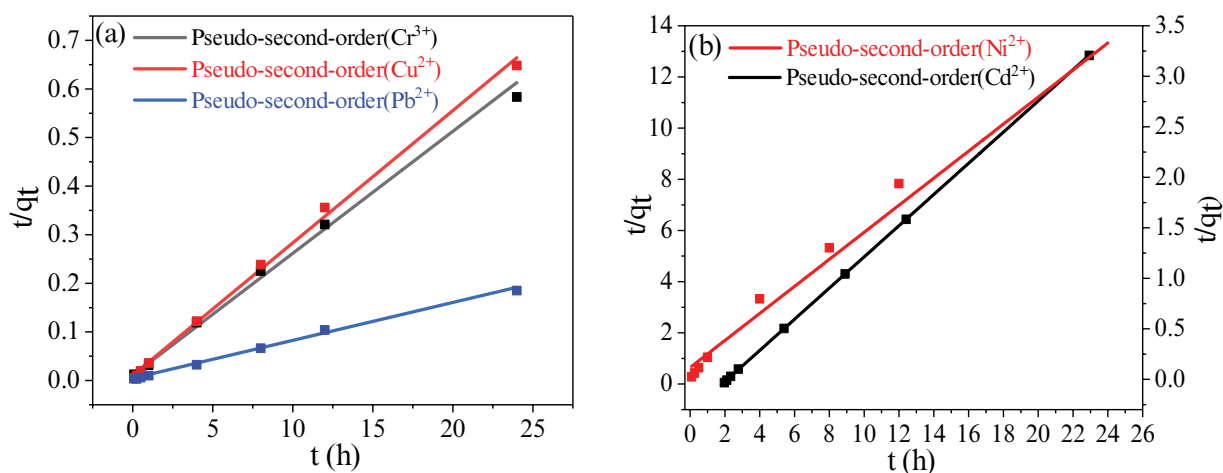


Fig. 4. (a and b) Pseudo-second-order kinetic for adsorption capacity on WPC600.

Table 4
Kinetic adsorption parameters of metal ions on WPC600

Ions	Pseudo-first-order				Pseudo-second-order		
	$q_{e,exp}$ (mg/g)	$q_{e,cal}$ (mg/g)	k_1 (1/h)	R^2	$q_{e,cal}$ (mg/g)	k_2 (g/(mg h))	R^2
Cr ³⁺	41.15	37.00	5.20	0.6605	39.84	0.059	0.9808
Ni ²⁺	7.58	10.88	5.66	0.2581	7.47	0.154	0.9946
Cu ²⁺	37.03	32.12	6.02	0.7134	36.74	0.067	0.9557
Cd ²⁺	1.97	1.78	28.86	0.1711	1.87	9.860	0.9709
Pb ²⁺	129.70	114.64	3.08	0.8858	128.21	0.013	0.9656

Table 5
Comparison of kinetic adsorption capacities with different adsorbents for Cu²⁺ and Pb²⁺

Adsorbent	$q_{e,cal}$ (Cu ²⁺) (mg/g)	References	Adsorbent	$q_{e,cal}$ (Pb ²⁺) (mg/g)	References
WPC600	36.74	This study	WPC600	128.21	This study
Date seeds	9.6	[31]	Fresh banana peels	14.88	[25]
Sewage sludge	7.32	[32]	Dehydrated banana peels	15.11	[25]
EMBC-400	18.33	[23]	Water hyacinths	47.33	[39]
E	29.6	[33]	Sugar cane bagasse	45.80	[40]
EW	95.2	[33]	MBC400	96.5	[41]
<i>Prosopis africana</i> shell	31.3	[34]	PBC400	56.9	[41]
Wheat straw	4.3	[35]	<i>Alternanthera philoxeroides</i>	52.55	[42]
Pigeon peas hulls	20.8	[36]	Sewage sludge	30.88	[43]
Pinewood	3.9	[37]	Activated carbon (<i>Polygonum orientale</i> Linn)	102.02	[44]
Orange peel	3.65	[38]	Orange peel	7.75	[38]

by X-ray photoelectron spectroscopy (XPS). The original major O1s curves shown in Fig. 5 could be fitted to three peaks, including C=O at 531.0 eV, C–O (aliphatic) at 532.2 eV, and C–O (aromatic) at 533.4 eV. In addition, according to the area of the corresponding peaks, the contents of C–O (aliphatic) and C–O (aromatic) groups are reduced from 40.00% and 39.52% to 37.25% and 31.21%, respectively (shown in Table 6), while C=O increasing from 15.28% to

27.18% after adsorption. It indicates that the C–O groups may be consumed by the metal ions adherence and C–H is converted to C=O functional groups during the interaction between semi-coke and heavy metal ions, which is proved that the surface oxidation degree of semi-coke increases due to the adsorption of heavy metal [45].

The peak fitting for N1s spectra of semi-coke were shown in Fig. 6 and five peaks were observed

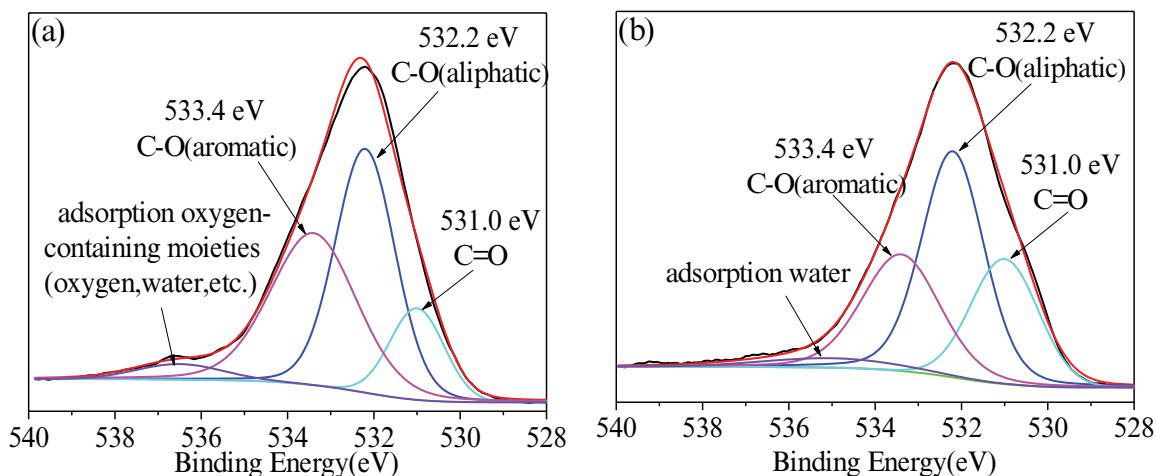


Fig. 5. Peak fitting for O1s spectra of semi-coke before (a) and after (b) adsorption of heavy metal ions.

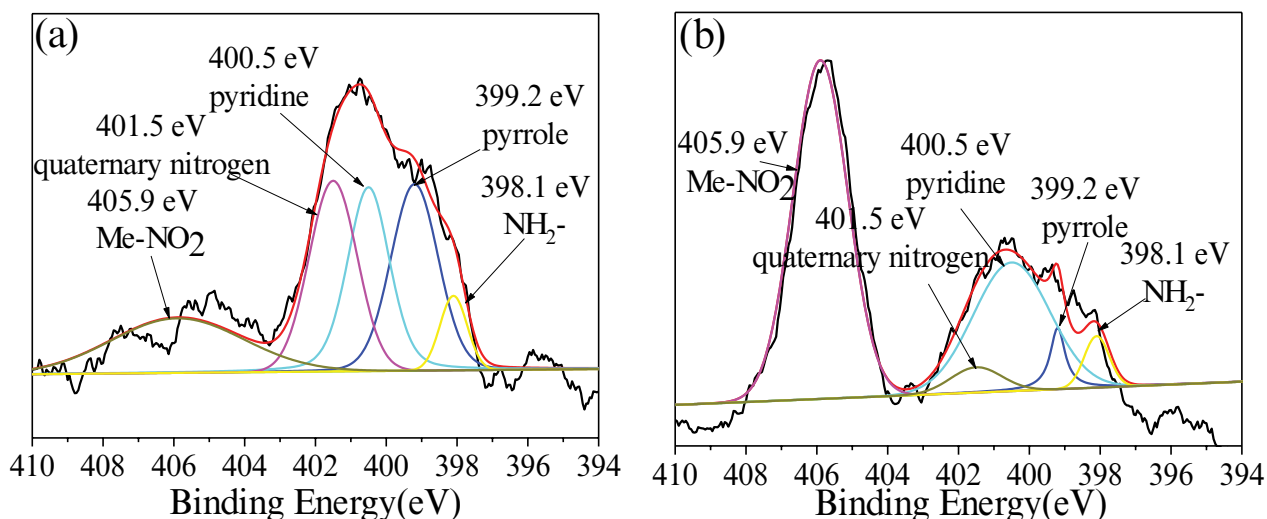
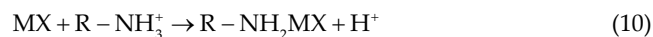
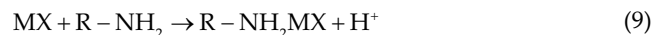


Fig. 6. Peak fitting for N1s spectra of semi-coke (a) before and (b) after adsorption of heavy metal ions.

including MeNO₂ at 405.9 eV, quaternary nitrogen at 401.5 eV, pyridine at 400.5 eV, pyrrole at 399.2 eV, and NH₂⁻ at 398.1 eV. The relative abundances (Table 6) indicate that the contents of pyridine and pyrrole significantly decrease from 24.18% and 23.54% to 6.90% and 19.65% after the adsorption, while the contents of MeNO₂ and quaternary nitrogen increase from 19.3% and 27.45% to 30.93% and 42.52%. The results suggest that nitrogen element of semi-coke in the form of pyridine and pyrrole is involved in the adsorption of heavy metal ions, eventually they are converted to MeNO₂ and quaternary nitrogen. In addition, NH₂⁻ also significantly decreases to 0.01% after adsorption, and NH₂ group may undergo the following reactions in the adsorption process [34]. Due to the electrical attraction between the nitrogen atom and the heavy metal ion is stronger than that of H⁺ ion, the combination between heavy metal ions and nitrogen of semi-coke may be considered much stronger [24].



where MX represents the heavy metal ions on semi-coke surface.

The S2p spectra before and after adsorption are given in Fig. 7. The peak at 163–165 eV is attributed to oxidative sulfur and 165–175 eV belongs to reduced sulfur. The S2p spectra could be fitted to three peaks, including S²⁻ at 169.1 eV, sulfate at 168.3 eV, and thiophene at 163.9 eV. As shown in Table 6, the contents of thiophene and S²⁻ reduce from 12.00% and 83.51% to 10.04% and 72.28% relatively. It indicates that sulfur of semi-coke in the two forms are

Table 6
Relative abundance of chemical bonds occurring modes in semi-coke before and after adsorption heavy metal ions

Chemical bond type	Before adsorption relative contents (%)	After adsorption relative contents (%)	Chemical bond type	Before adsorption relative contents (%)	After adsorption relative contents (%)
C=O	15.28	27.18	Pyridine	23.54	19.65
C–O (aliphatic)	40.00	37.25	Quaternary nitrogen	27.45	42.52
C–O (aromatic)	39.52	31.21	MeN _o 2	19.13	30.93
Inorganic oxygen	5.21	4.36	S ²⁻	83.51	72.28
NH ₂ -	5.71	0.01	Thiophene	12.00	10.04
Pyrrole	24.18	6.90	Sulfate	4.49	17.67

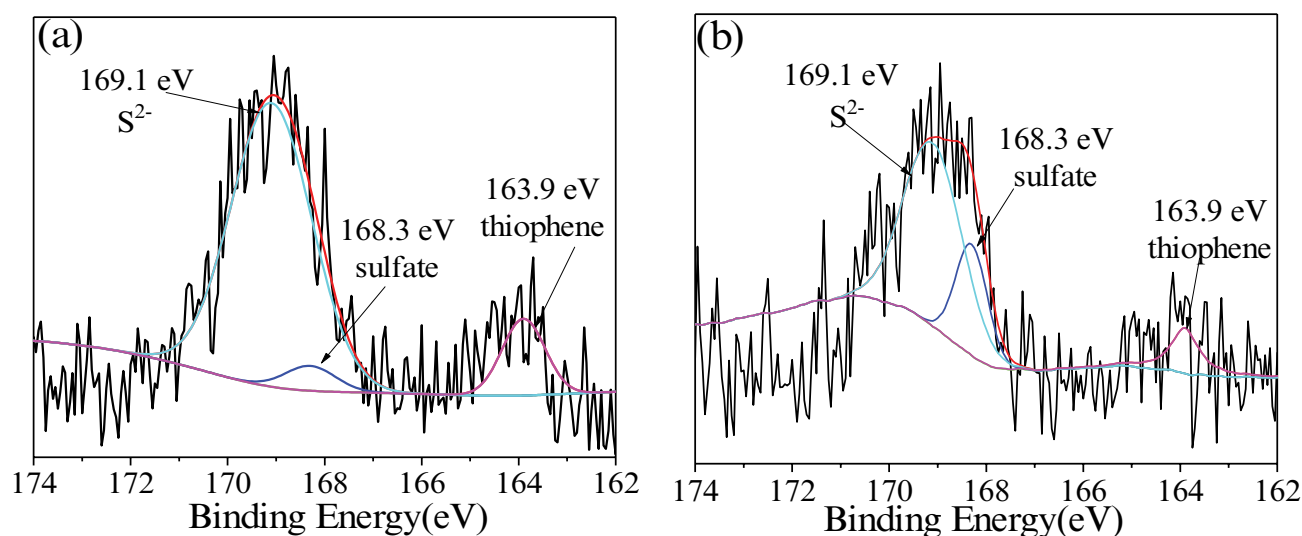


Fig. 7. Peak fitting for S2p spectra of semi-coke before (a) and after (b) adsorption of heavy metal ions.

involved in chemical reaction during adsorption process of heavy metal ions, resulting in forming sulfate group with obviously increasing from 4.49% to 17.67%.

The main adsorption mechanism of heavy metal ions on the semi-coke could also be demonstrated, combining with the Cu2p, Cd3d, and Ni2p XPS spectra shown in Fig. 8. The Cu2p XPS spectra after adsorption given in Fig. 8a could be fitted to three peaks, including Cu2p_{1/2} at 953.6 eV, Cu2p_{3/2} at 934.7 eV, and Cu2p_{3/2} at 933.8 eV. The existing forms of Cu corresponding to those peaks belong to CuO and Cu(OH)₂ precipitates. The above results show that precipitation would occur between semi-coke and Cu²⁺ in solution, and probably copper oxide and hydroxide could be responsible for Cu²⁺ adsorption. The Cd3d spectra after adsorption shown in Fig. 8b could be fitted to two peaks. The peaks appeared at the binding energy of 405.1 and 411.9 eV, which gives the existence of Cd3d_{5/2} and Cd3d_{3/2} respectively. The two binding energies correspond to the existing forms of Cd²⁺, and the corresponding substances are CdO precipitates [46]. In addition, the Ni2p spectrum after adsorption given in Fig. 8c could be fitted to two peaks, including Ni2p_{1/2} at 874.3 eV, Ni2p_{3/2} at 856.4 eV. The

existing form of Ni corresponding to two peaks is Ni(OH)₂. The value of spin separation energy between the two peaks is 17.9 eV, which is larger than that of Ni(OH)₂ (17.65 eV), indicating the formed Ni(OH)₂ precipitates is relatively stable and not easy to dissociate [47].

The adsorption mechanism of the as-obtained semi-coke adsorbent for heavy metals in solution is very complex, including electrostatic attraction, chemical interaction between functional groups on surface of semi-coke and heavy metal ions, surface precipitation in the whole adsorption process, but chemical interaction is more crucial for the metal ions adsorption [29,48]. Guo et al. [49] studied the effect of porosity, specific surface area, and surface functional groups of carbonaceous materials on heavy metal ions adsorption and found the role of chemical interaction. In this study, XPS analysis confirms that the strongly basic surface N-containing and acidic surface O-containing functional groups of semi-coke improve the adsorption of heavy metal ions through cation exchange and being surface precipitation. A great amount of surface functional groups of semi-coke leads to increasing the adsorption ability for metal ions.

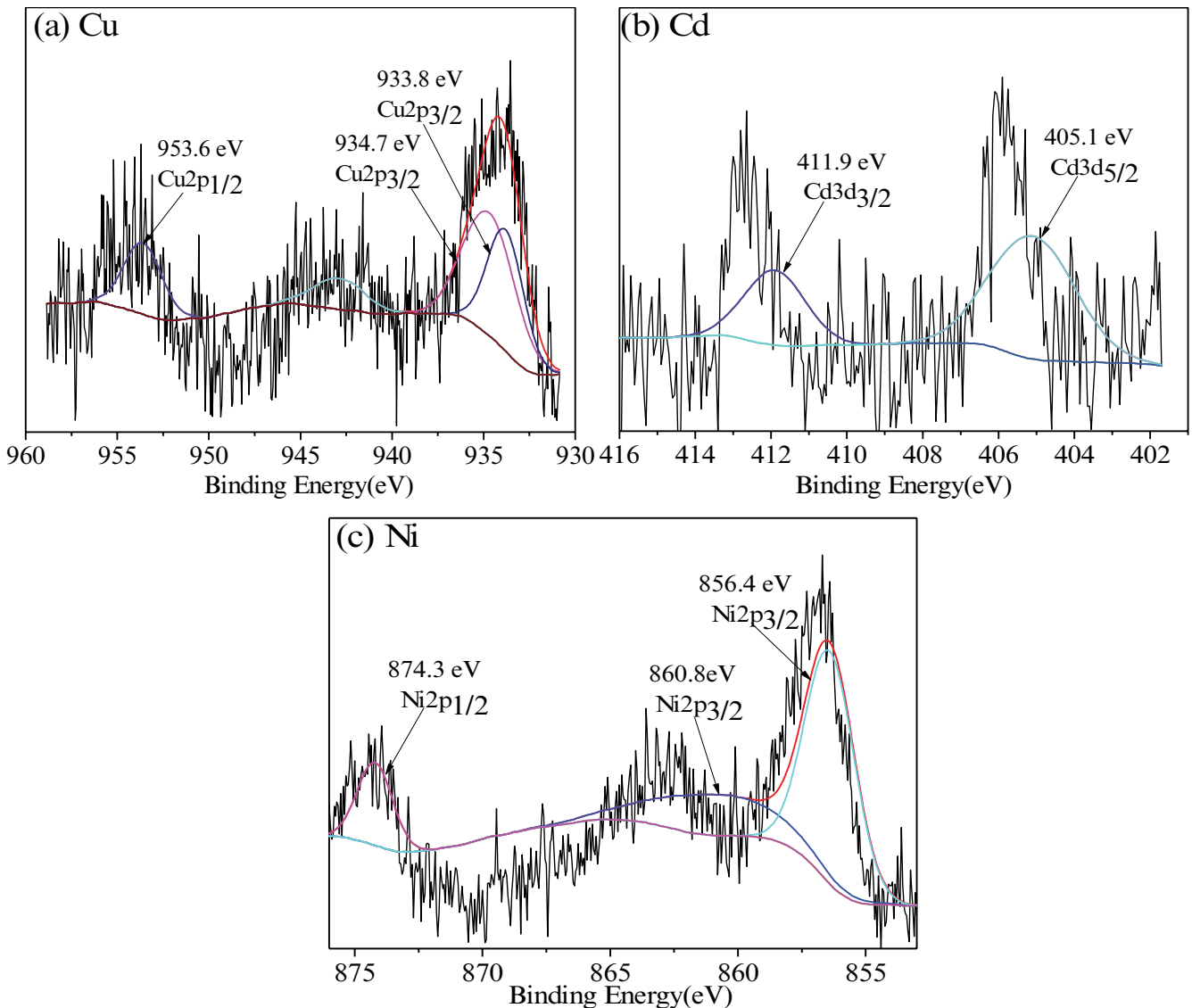


Fig. 8. (a) Cu2p, (b) Cd3d, and (c) Ni2p spectra of semi-coke after adsorption heavy metal ions.

4. Conclusion

Semi-coke is a kind of by-product from the procedure of coal pyrolysis and the power for adsorption of Cr^{3+} , Ni^{2+} , Cu^{2+} , Cd^{2+} , and Pb^{2+} ions from water solution was investigated. The adsorption thermodynamics matched the Freundlich model, namely adsorption of metal ions mainly occurring on non-uniform surface of the semi-coke. Adsorption kinetics confirmed to the pseudo-second-order model, indicating chemisorption. WPC600 from pyrolysis of coal at 600°C with higher surface functional groups shows a better adsorption capacity for the heavy metals, especially for aqueous solutions containing Cu^{2+} and Pb^{2+} . XPS analyze suggested that adsorption mechanism was through the chemical interaction between surface functional groups (such as C–O, NH_2^- , pyridine, pyrrole, and thiophene) and metal ions in the adsorption process. These results will provide a promising method to produce effective adsorbent

from coal for the removal heavy metal ions and it may have great ecological and environmental significance.

Acknowledgments

The authors wish to acknowledge to the financial support of the Fundamental Research Funds for the Central Universities (Grant No. 2019XKQYMS14).

References

- [1] L. Joseph, B.M. Jun, J.R.V. Flora, C.M. Park, Y. Yoon, Removal of heavy metals from water sources in the developing world using low-cost materials: a review, *Chemosphere*, 229 (2019) 142–159.
- [2] K.H. Vardhan, P.S. Kumar, R.C. Panda, A review on heavy metal pollution, toxicity and remedial measures: current trends and future perspectives, *J. Mol. Liq.*, 290 (2019) 111197, doi: 10.1016/j.molliq.2019.111197.

- [3] X. Song, P. Gunawan, R. Jiang, S.S.J. Leong, K. Wang, R. Xu, Surface activated carbon nanospheres for fast adsorption of silver ions from aqueous solutions, *J. Hazard. Mater.*, 194 (2011) 162–168.
- [4] D. Kim, J. Min, J.Y. Yoo, J.W. Park, *Eisenia fetida* growth inhibition by amended activated carbon causes less bioaccumulation of heavy metals, *J. Soils Sediments*, 14 (2014) 1766–1773.
- [5] L.Y. Li, X. Gong, O. Abida, Waste-to-resources: exploratory surface modification of sludge-based activated carbon by nitric acid for heavy metal adsorption, *Waste Manage.*, 87 (2019) 375–386.
- [6] L. Wang, Y. Wang, F. Ma, V. Tankpa, S. Bai, X. Guo, X. Wang, Mechanisms and reutilization of modified biochar used for removal of heavy metals from wastewater: a review, *Sci. Total Environ.*, 668 (2019) 1298–1309.
- [7] B.J. Ni, Q.S. Huang, C. Wang, T.Y. Ni, J. Sun, W. Wei, Competitive adsorption of heavy metals in aqueous solution onto biochar derived from anaerobically digested sludge, *Chemosphere*, 219 (2019) 351–357.
- [8] F. Xiao, J. Cheng, W. Cao, C. Yang, J. Chen, Z. Luo, Removal of heavy metals from aqueous solution using chitosan-combined magnetic biochars, *J. Colloid Interface Sci.*, 540 (2019) 579–584.
- [9] H. Zhang, J. Chen, P. Liang, L. Wang, Mercury oxidation and adsorption characteristics of potassium permanganate modified lignite semi-coke, *Environ. Sci.*, 24 (2012) 2083–2090.
- [10] W.T. Wang, C.H. Li, Z.F. Yan, Study on molding semi-coke used for flue-gas desulphurization, *Catal. Today*, 158 (2010) 235–240.
- [11] Z. Yan, L.L. Liu, Y.L. Zhang, J.P. Liang, J.P. Wang, Z.T. Zhang, X.D. Wang, Activated semi-coke in SO₂ removal from flue gas: selection of activation methodology and desulfurization mechanism study, *Energy Fuels*, 27 (2013) 3080–3089.
- [12] K. Zhang, Y. He, Z. Wang, T. Huang, Q. Li, S. Kumar, K. Cen, Multi-stage semi-coke activation for the removal of SO₂ and NO, *Fuel*, 210 (2017) 738–747.
- [13] W. Yang, C. Li, L. Wang, S.N. Sun, X. Yan, Solvothermal fabrication of activated semi-coke supported TiO₂-rGO nanocomposite photocatalysts and application for NO removal under visible light, *Appl. Surf. Sci.*, 353 (2015) 307–316.
- [14] H.W. Zhang, X.L. Li, L. Wang, P. Liang, Characteristics and stability of mercury vapor adsorption over two kinds of modified semicoke, *Sci. World J.*, 2014 (2014) 260141, doi: 10.1155/2014/260141.
- [15] L. Zhang, Z. Liu, Y. Fan, A. Fan, X. Han, Modification of semi-coke powder and its adsorption mechanisms for Cr(VI) and methylene blue, *IOP Conf. Ser.: Earth Environ. Sci.*, 121 (2018) 022024, doi: 10.1088/1755-1315/121/2/022024.
- [16] H.P. Boehm, Some aspects of the surface chemistry of carbon blacks and other carbons, *Carbon*, 32 (1994) 759–769.
- [17] C. Ma, C. Zou, J. Zhao, R. Shi, X. Li, J. He, X. Zhang, Pyrolysis characteristics of low-rank coal under a CO-containing atmosphere and properties of the prepared coal chars, *Energy Fuels*, 33 (2019) 6098–6112.
- [18] L. Zhang, S. Qi, N. Takeda, S. Kudo, J. Hayashi, K. Norinaga, Characteristics of gas evolution profiles during coal pyrolysis and its relation with the variation of functional groups, *Int. J. Coal Sci. Technol.*, 5 (2018) 452–463.
- [19] G.J. Shang, C.H. Li, M.Q. Miao, Z. Yang, Surface characterization and SO₂ removal activity of activated semi-coke with heat treatment, *New Carbon Mater.*, 23 (2008) 37–43.
- [20] C.P. Ye, H.J. Huang, X.H. Li, W.Y. Li, J. Feng, The oxygen evolution during pyrolysis of HunlunBuir lignite under different heating modes, *Fuel*, 207 (2017) 85–92.
- [21] S. Sato, K. Yoshihara, K. Moriyama, M. Machida, H. Tatsumoto, Influence of activated carbon surface acidity on adsorption of heavy metal ions and aromatics from aqueous solution, *Appl. Surf. Sci.*, 253 (2007) 8554–8559.
- [22] L. Zhang, W. Li, H. Cao, D. Hu, X. Chen, Y. Guan, J. Tang, H. Gao, Ultra-efficient sorption of Cu²⁺ and Pb²⁺ ions by light biochar derived from *Medulla tetrapanacis*, *Bioresour. Technol.*, 291 (2019) 121818, doi: 10.1016/j.biortech.2019.121818.
- [23] J. Xu, X. Lv, J. Li, Y. Li, L. Shen, H. Zhou, X. Xu, Simultaneous adsorption and dechlorination of 2,4-dichlorophenol by Pd/Fe nanoparticles with multi-walled carbon nanotube support, *J. Hazard. Mater.*, 225 (2012) 36–45.
- [24] B. Zhou, Z. Wang, D. Shen, F. Shen, C. Wu, R. Xiao, Low cost earthworm manure-derived carbon material for the adsorption of Cu²⁺ from aqueous solution: impact of pyrolysis temperature, *Ecol. Eng.*, 98 (2017) 189–195.
- [25] N. Zhou, H. Chen, J. Xi, D. Yao, Z. Zhou, Y. Tian, X. Lu, Biochars with excellent Pb(II) adsorption property produced from fresh and dehydrated banana peels via hydrothermal carbonization, *Bioresour. Technol.*, 232 (2017) 204–210.
- [26] P. Nanta, K. Kasemwong, W. Skolpap, Isotherm and kinetic modeling on superparamagnetic nanoparticles adsorption of polysaccharide, *J. Environ. Chem. Eng.*, 6 (2018) 794–802.
- [27] M.J. Moon, M.S. Jhon, The studies on the hydration energy and water structures in dilute aqueous solution, *Bull. Chem. Soc. Jpn.*, 59 (1986) 1215–1222.
- [28] V. Vimonses, S. Lei, B. Jin, C.W.K. Chow, C. Saint, Kinetic study and equilibrium isotherm analysis of Congo Red adsorption by clay materials, *Chem. Eng. J.*, 148 (2009) 354–364.
- [29] M. Matouq, N. Jildeh, M. Qtaishat, M. Hindiye, M.Q.A. Syouf, The adsorption kinetics and modeling for heavy metals removal from wastewater by *Moringa pods*, *J. Environ. Chem. Eng.*, 37 (2015) 75–784.
- [30] L.P. Zhang, H. Song, K. Xu, L. Jiang, Y. Wang, S. Su, Y.M. Xiao, L.Y. Shan, W.L. Shen, H.F. Li, G. Chen, H. Tang, Study on the structural evolution of semi-chars and their solvent extracted materials during pyrolysis process of a Chinese low-rank coal, *Fuel*, 214 (2018) 363–368.
- [31] Z. Mahdi, Q.J. Yu, A. El-Hanandeh, Investigation of the kinetics and mechanisms of nickel and copper ions adsorption from aqueous solutions by date seed derived biochar, *J. Environ. Chem. Eng.*, 6 (2018) 1171–1181.
- [32] T. Shen, Y. Tang, X.-Y. Lu, Z. Meng, Mechanisms of copper stabilization by mineral constituents in sewage sludge biochar, *J. Cleaner Prod.*, 193 (2018) 185–193.
- [33] B.S. Kim, H.W. Lee, S.H. Park, K. Baek, J.K. Jeon, H.J. Cho, S.C. Jung, S.C. Kim, Y.K. Park, Removal of Cu²⁺ by biochars derived from green macroalgae, *Environ. Sci. Pollut. Res. Int.*, 23 (2016) 985–994.
- [34] S.E. Elaigwu, V. Rocher, G. Kyriakou, G.M. Greenway, Removal of Pb²⁺ and Cd²⁺ from aqueous solution using chars from pyrolysis and microwave-assisted hydrothermal carbonization of *Prosopis africana* shell, *J. Ind. Eng. Chem.*, 20 (2014) 3467–3473.
- [35] M. Gorgievskia, D. Božića, V. Stankovičb, N. Štrbacb, S. Šerbulab, Kinetics, equilibrium and mechanism of Cu²⁺, Ni²⁺ and Zn²⁺ ions biosorption using wheat straw, *Ecol. Eng.*, 58 (2013) 113–122.
- [36] D.K. Venkata Ramana, K.R.D. Harikishore, J.S. Yu, K. Seshaiyah, Pigeon peas hulls waste as potential adsorbent for removal of Pb(II) and Ni(II) from water, *Chem. Eng. J.*, 197 (2012) 24–33.
- [37] Z. Liu, F.S. Zhang, Removal of lead from water using biochars prepared from hydrothermal liquefaction of biomass, *J. Hazard. Mater.*, 167 (2009) 933–939.
- [38] G. Annadurai, R.S. Juang, D.J. Lee, Adsorption of heavy metals from water using banana and orange peels, *Water Sci. Technol.*, 47 (2003) 185–190.
- [39] Y. Ding, Y. Liu, S. Liu, Z. Li, X. Tan, X. Huang, G. Zeng, Y. Zhou, B. Zheng, X. Cai, Competitive removal of Cd(II) and Pb(II) by biochars produced from water hyacinths: performance and mechanism, *RSC Adv.*, 6 (2016) 5223–5232.
- [40] A.A. Abdelhafez, J. Li, Removal of Pb(II) from aqueous solution by using biochars derived from sugar cane bagasse and orange peel, *J. Taiwan Inst. Chem. Eng.*, 61 (2016) 367–375.
- [41] Z. Wang, G. Liu, H. Zheng, F. Li, H.H. Ngo, W. Guo, C. Liu, L. Chen, B. Xing, Investigating the mechanisms of biochar's removal of lead from solution, *Bioresour. Technol.*, 177 (2015) 308–317.
- [42] Y. Yang, Z. Wei, X. Zhang, X. Chen, D. Yue, Q. Yin, L. Xiao, L. Yang, Biochar from *Alternanthera philoxeroides* could remove Pb(II) efficiently, *Bioresour. Technol.*, 171 (2014) 227–232.
- [43] B. Lu, W. Zhang, Y. Yang, X. Huang, S. Wang, R. Qiu, Relative distribution of Pb²⁺ sorption mechanisms by sludge-derived biochar, *Water Res.*, 46 (2012) 854–862.

- [44] L. Wang, J. Zhang, R. Zhao, Y. Li, C. Li, C. Zhang, Adsorption of Pb(II) on activated carbon prepared from *Polygonum orientale* Linn.: kinetics, isotherms, pH, and ionic strength studies, *Bioresour. Technol.*, 101 (2010) 5808–5814.
- [45] N.H. Hsu, S.L. Wang, Y.H. Liao, S.T. Huang, Y.M. Tzou, Y.M. Huang, Removal of hexavalent chromium from acidic aqueous solutions using rice straw-derived carbon, *J. Hazard. Mater.*, 171 (2009) 1066–1070.
- [46] P. Mao, L. Qi, X. Liu, L. Liu, Y. Jiao, S.W. Chen, L. Yang, Synthesis of Cu/Cu₂O hydrides for enhanced removal of iodide from water, *J. Hazard. Mater.*, 328 (2017) 21–28.
- [47] X.L. Zhao, Y. Wang, H.Y. Wu, P. Li, Insights into the effect of humic acid on Ni(II) sorption mechanism on illite: batch, XPS and EXAFS investigations, *J. Mol. Liq.*, 248 (2017) 1030–1038.
- [48] M. Barczak, K. Michalak-Zwierz, K. Gdula, K. Tyszczyk-Rotko, R. Dobrowolski, A. Dąbrowski, Ordered mesoporous carbons as effective sorbents for removal of heavy metal ions, *Microporous Mesoporous Mater.*, 211 (2015) 162–173.
- [49] Z. Guo, J. Fan, J. Zhang, Y. Kang, H. Liu, L. Jiang, C. Zhang, Sorption heavy metal ions by activated carbons with well-developed microporosity and amino groups derived from *Phragmites australis* by ammonium phosphates activation, *J. Taiwan Inst. Chem. Eng.*, 58 (2009) 290–296.